J|A|C|S ARTICLES

Published on Web 05/25/2009

Palladium Nanoparticles on Graphite Oxide and Its Functionalized Graphene Derivatives as Highly Active Catalysts for the Suzuki−Miyaura Coupling Reaction

Gil M. Scheuermann,[†] Luigi Rumi,[‡] Peter Steurer,[†] Willi Bannwarth,[‡] and Rolf Mülhaupt[†,§,*]

Freiburger Materialforschungszentrum (FMF) and Institut für Makromolekulare Chemie, Albert-Ludwigs-Universität Freiburg, Stefan-Meier Strasse 21-31, D-79104 Freiburg, Germany, Institut für Organische Chemie und Biochemie, Albert-Ludwigs-Universität Freiburg, Albertstrasse 21, D-79104 Freiburg, Germany, and Freiburg Institute for Advanced Studies (FRIAS), Soft Matter Research, Albertstrasse 19, D-79104 Freiburg, Germany

Received February 20, 2009; E-mail: rolf.muelhaupt@fmf.uni-freiburg.de

Abstract: Pd^{2+}-exchanged graphite oxide and chemically derived graphenes therefrom were employed as supports for Pd nanoparticles. The influence of catalyst preparation, carbon functionalization, and catalyst morphology on the catalytic activity in the Suzuki−Miyaura coupling reactions was investigated. The catalysts were characterized by means of spectroscopy (FT-IR, solid-state ^{13}C NMR, AAS, XPS), X-ray scattering (WAXS), surface area analysis (BET, methylene blue adsorption), and electron microscopy (TEM, ESEM). In contrast to the conventional Pd/C catalyst, graphite oxide and graphene-based catalysts gave much higher activities with turnover frequencies exceeding 39 000 h^{-1}, accompanied by very low palladium leaching (<1 ppm).

Introduction

During the last few years, graphite oxide (GO)[1,2] and chemically derived graphene (CDG)[3] have been rediscovered as extremely versatile carbon materials. This renaissance is mainly due to its importance in nanosciences (e.g., as a low-cost alternative to carbon nanotubes in polymer nanocomposites[4] and as hydrogen storage materials[5] or in nanoelectronics as insulating material or semiconductor).[6]

GO is easily available by controlled chemical or electrochemical oxidation of graphite via its nitrate or hydrogensulfate salts.[7−10] It is a nonstoichiometric hygroscopic compound, and different models have been proposed concerning its structure and composition.[11−14] According to more recent studies, the layered structure is preserved as the partial oxidation produces sheets with graphitic domains and crumpled regions where epoxide and hydroxyl groups are located on the basal planes

[†] FMF and Institut für Makromolekulare Chemie, Albert-Ludwigs-Universität Freiburg.

[‡] Institut für Organische Chemie und Biochemie, Albert-Ludwigs-Universität Freiburg.

[§] FRIAS.

(1) (a) Ajayan, P. M.; Yakobson, B. I. *Nature* **2006**, *441*, 818–819. (b) Dikin, D. A.; Stankovich, S.; Zimney, E. J.; Piner, R. D.; Dommett, G. H. B.; Evmenenko, G.; Nguyen, S. T.; Ruoff, R. S. *Nature* **2007**, *448*, 457–460. (c) Prud'homme, R. K.; Aksay, I. A.; Adamson, D. H.; Abdala, A. A. U.S. Patent 092432, 2007. (d) Ruoff, R. *Nat. Nanotechnol.* **2008**, *3*, 10–11.

(2) McAllister, M. J.; Li, J.-L.; Adamson, D. H.; Schniepp, H. C.; Abdala, A. A.; Liu, J.; Herrera-Alonso, M.; Milius, D. L.; Car, R.; Prud'homme, R. K.; Aksay, I. A. *Chem. Mater.* **2007**, *19*, 4396–4404.

(3) (a) Stankovich, S.; Dikin, D. A.; Dommett, G. H. B.; Kohlhaas, K. M.; Zimney, E. J.; Stach, E. A.; Piner, R. D.; Nguyen, S. T.; Ruoff, R. S. *Nature* **2006**, *442*, 282–286. (b) Geim, A. K.; Novoselov, K. S. *Nat. Mater.* **2007**, *6*, 183–191. (c) Li, D.; Kaner, R. B. *Science* **2008**, *320*, 1170–1171.

(4) (a) Ramanathan, T.; Abdala, A. A.; Stankovich, S.; Dikin, D. A.; Herrera-Alonso, M.; Piner, R. D.; Adamson, D. H.; Schniepp, H. C.; Chen, X.; Ruoff, R. S.; Nguyen, S. T.; Aksay, I. A.; Prud'homme, R. K.; Brinson, L. C. *Nat. Nanotechnol.* **2008**, *3*, 327–331. (b) Ramanathan, T.; Stankovich, S.; Dikin, D. A.; Liu, H.; Shen, H.; Nguyen, S. T.; Brinson, L. C. *J. Polym. Sci., Part B: Polym. Phys.* **2007**, *45*, 2097–2112. (c) Liu, P. G.; Gong, K. C.; Xiao, P.; Xiao, M. *J. Mater. Chem.* **2000**, *10*, 933–935. (d) Uhl, F. M.; Wilkie, C. A. *Polym. Degrad. Stab.* **2004**, *84*, 215–226.

(5) Matsuo, Y.; Kume, K.; Fukutsuda, T.; Sugie, Y. *Carbon* **2003**, *41*, 2167–2169.

(6) (a) Eda, G.; Fanchini, G.; Chhowalla, M. *Nat. Nanotechnol.* **2008**, *3*, 270–274. (b) Berger, C.; Song, Z.; Li, X.; Wu, X.; Brown, N.; Naud, C.; Mayou, D.; Li, T.; Hass, J.; Marchenkov, A. N.; Conrad, E. H.; First, P. N.; de Heer, W. A. *Science* **2006**, *312*, 1191–1196. (c) Freitag, M. *Nat. Nanotechnol.* **2008**, *3*, 455–457. (d) Wang, X.; Zhi, L.; Müllen, K. *Nano Lett.* **2008**, *8*, 323–327.

(7) (a) Brodie, B. C. *Ann. Chim. Phys.* **1860**, *59*, 466–472. (b) Staudenmaier, L. *Ber. Dtsch. Chem. Ges.* **1898**, *31*, 1481–1487. (c) Titelman, G. I.; Gelman, V.; Bron, S.; Khalfin, R. L.; Cohen, Y.; Bianco-Peled, H. *Carbon* **2005**, *43*, 641–649.

(8) Hummers, W. S.; Offemann, R. E. *J. Am. Chem. Soc.* **1958**, *80*, 1339.

(9) Boehm, H.-P.; Scholz, W. *Liebigs Ann. Chem.* **1965**, *691*, 1–8.

(10) (a) Boehm, H.-P.; Eckel, M.; Scholz, W. *Z. Anorg. Allg. Chem.* **1967**, *353*, 236–242. (b) Nakajima, T.; Matsuo, Y. *Carbon* **1994**, *32*, 469–475.

(11) (a) Hofmann, U.; Frenzel, A.; Wilm, D.; Csalan, E. *Kolloid-Z.* **1932**, *61*, 297–304. (b) Hofmann, U.; Frenzel, A.; Csalan, E. *Liebigs Ann. Chem.* **1934**, *510*, 1–41.

(12) Clauss, A.; Plass, R.; Boehm, H.-P.; Hofmann, U. *Z. Anorg. Allg. Chem.* **1957**, *291*, 205–220.

(13) (a) Ruess, G. *Kolloid-Z.* **1945**, *110*, 17–26. (b) Ruess, G.; Vogt, F. *Monatsh. Chem.* **1948**, *78*, 222–242.

(14) (a) Beckett, R. J.; Croft, R. C. *J. Phys. Chem.* **1952**, *56*, 929–941. (b) Cassagneau, T.; Guerin, F.; Fendler, J. H. *Langmuir* **2000**, *16*, 7318–7324. (c) Hontoria-Lucas, C.; López-Peinado, A. J.; López-González, J. D.; Rojas-Cervantes, M. L.; Martín-Aranda, R. M. *Carbon* **1995**, *33*, 1585–1592. (d) Nakajima, T.; Mabuchi, A.; Hagiwara, R. *Carbon* **1988**, *26*, 357–361.

 10.1021/ja901105a CCC: $40.75

and carbonyl and carboxyl groups are placed at the edges.[15,16] Thermal or chemical reduction of GO leads to an expanded graphite or even exfoliated graphitic nanoplatelets and CDG sheets, respectively.[2,17−19]

Because of the functional groups present in GO, the sorption and intercalation of ions and molecules is possible.[12,20] This feature, together with the high specific surface area of GO and CDG of 400 $m^2\ g^{-1}$ up to 1500 $m^2\ g^{-1}$, makes them promising materials for catalytic applications.[2,21] To date, there are only a few examples of GO-based materials as catalysts.[21−23] More than 50 years ago, Boehm et al. investigated the chemistry of GO in depth and used different methods for the determination of the specific surface of CDG inter alia the catalytic production of HBr.[21] Later, in a USSR patent, Titelman et al. described the deposition of NiO and CuO by thermal reduction of metal amine precursors on a GO support as a catalyst for removing oxygen impurities from industrial gases.[22] At the same time, Kyotani et al. synthesized carbon−metal composites by thermal treatment of Na^+, Ca^{2+}, Cu^{2+}, and Fe^{2+}-exchanged graphite oxide.[24] Although they did not describe any catalytic applications, they characterized the obtained materials in detail and observed a magnetic anisotropy for the Fe sample. Kovtyukhova and co-workers investigated the intercalation of different transition-metal complexes in GO.[25] They also synthesized nanometer-sized clusters of Cu and Ni in a layered carbon matrix by thermal breakdown of their intercalated GOs but did not test the catalytic performance of these materials.[26] Mastalir et al. were the first to determine the high catalytic activity and selectivity of their nano-Pd/GO systems in liquid-phase hydrogenation of alkynes.[23] Ion exchange of GO with a Pd complex and subsequent reduction to nanosized crystallites by H_2 resulted in a catalyst that surpassed the activity of commercial supported Pd catalysts such as Pd on activated carbon (Pd/C) and Pd graphimet. The latter is a rather uncommon catalyst synthesized by slow intercalation of $PdCl_2$ into graphite in a chlorine atmosphere with subsequent reduction to Pd nanoparticles.[27]

Several Pd nanoparticle catalysts for C−C coupling reactions such as the Mizoroki−Heck reaction[28] and the Suzuki−Miyaura reaction[29] have been described in the literature.[30−32] Immobilization or stabilization procedures of Pd nanoparticles in ionic liquids,[33] polymers,[34] organic−inorganic fluorinated hybrid materials,[35] and glass−polymer composite materials[36] as well as on common inorganic substrates such as carbon,[37−40] silica,[41] alumina,[42] or zeolites[43] are known to yield active catalysts for C−C coupling reactions.

In the present study, we exploit GO and its CDG derivatives as a support for palladium clusters and nanoparticles. The Suzuki−Miyaura reaction has been selected as model reaction for evaluating GO- and CDG-based palladium catalysts.

(15) Lerf, A.; He, H. Y.; Forster, M.; Klinowski, J. *J. Phys. Chem. B* **1998**, *102*, 4477–4482.

(16) (a) Boukhvalov, D. W.; Katsnelson, M. I. *J. Am. Chem. Soc.* **2008**, *130*, 10697–10701. (b) Kudin, K. N.; Ozbas, B.; Schniepp, H. C.; Prud'homme, R. K.; Aksay, I. A.; Car, R. *Nano Lett.* **2008**, *8*, 36–41.

(17) Schniepp, H. C.; Li, J.-L.; McAllister, M. J.; Sai, H.; Herrera-Alonso, M.; Adamson, D. H.; Prud'homme, R. K.; Car, R.; Saville, D. A.; Aksay, I. A. *J. Phys. Chem. B* **2006**, *110*, 8535–8539.

(18) (a) Boehm, H.-P.; Clauss, A.; Hofmann, U.; Fischer, G. O. *Z. Naturforsch.* **1962**, *17*, 150. (b) Bourlinos, A. B.; Gournis, D.; Petridis, D.; Szabó, T.; Szeri, A.; Dékány, I. *Langmuir* **2003**, *19*, 6050–6055. (c) Li, D.; Mueller, M. B.; Gilje, S.; Kaner, R. B.; Wallace, G. G. *Nat. Nanotechnol.* **2008**, *3*, 101–105.

(19) (a) Stankovich, S.; Piner, R. D.; Chen, X. Q.; Wu, N. Q.; Nguyen, S. T.; Ruoff, R. S. *J. Mater. Chem.* **2006**, *16*, 155–158. (b) Stankovich, S.; Dikin, D. A.; Piner, R. D.; Kohlhaas, K. A.; Kleinhammes, A.; Jia, Y.; Wu, Y.; Nguyen, S. T.; Ruoff, R. S. *Carbon* **2007**, *45*, 1558–1565.

(20) (a) Thiele, H. *Kolloid-Z.* **1937**, *80*, 1–20. (b) Slabaugh, W. H.; Seiler, B. C. *J. Phys. Chem.* **1962**, *66*, 396–401. (c) Dékány, I.; Krüger-Grasser, R.; Weiss, A. *Colloid Polym. Sci.* **1998**, *276*, 570–576.

(21) Boehm, H.-P.; Clauss, A.; Fischer, G. O.; Hofmann, U. *Z. Anorg. Allg. Chem.* **1962**, *316*, 119–127.

(22) Titelman, G. I.; Karamanenko, S. V.; Novikov, Y. N.; Gorozhankin, E. V.; Golosman, E. Z. (Novomoskovskij Gni I Pi Azotno SU, State Scientific Research and Planning Institute of the Nitrogen Industry and of Organic Synthesis USSR.). USSR Patent SU 1806005, 1993.

(23) (a) Mastalir, Á.; Király, Z.; Patzkó, Á.; Dékány, I.; L'Argentiere, P. *Carbon* **2008**, *46*, 1631–1637. (b) Mastalir, Á.; Király, Z.; Benko, M.; Dékány, I. *Catal. Lett.* **2008**, *124*, 34–38.

(24) Kyotani, T.; Suzuki, K.; Yamashita, H.; Tomita, A. *Tanso* **1993**, *160*, 255–265.

(25) Kovtyukhova, N. I.; Karpenko, G. A.; Chuiko, A. A. *Russ. J. Inorg. Chem.* **1992**, *37*, 566–569.

(26) Kovtyukhova, N. I. *Theor. Exp. Chem.* **1995**, *31*, 77–91.

(27) (a) Croft, R. C. *Aust. J. Chem.* **1956**, *9*, 184–193. (b) Ebert, L. B. *J. Mol. Catal.* **1982**, *15*, 275–296. (c) Lalancette, J.-M. (Ventron Corp.). U.S. Patent 3847963, 1974. (d) Mastalir, Á.; Notheisz, F.; Bartók, M.; Haraszti, T.; Király, Z.; Dékány, I. *Appl. Catal., A* **1996**, *144*, 237–248.

(28) (a) Beletskaya, I. P.; Cheprakov, A. V. *Chem. Rev.* **2000**, *100*, 3009–3066. (b) Heck, R. F. *Acc. Chem. Res.* **1979**, *12*, 146–151. (c) Heck, R. F.; Nolley, J. P., Jr. *J. Org. Chem.* **1972**, *37*, 2320–2322. (d) Mizoroki, T.; Mori, K.; Ozaki, A. *Bull. Chem. Soc. Jpn.* **1971**, *44*, 581–583. (e) Whitcombe, N. J.; Hii, K. K.; Gibson, S. E. *Tetrahedron* **2001**, *57*, 7449–7476.

(29) (a) Suzuki, A.; Miyaura, N. *J. Chem. Soc., Chem. Commun.* **1979**, 866–867. (b) Suzuki, A. *Pure Appl. Chem.* **1994**, *66*, 213–222. (c) Deng, Y.; Gong, L.; Mi, A.; Liu, H.; Jiang, Y. *Synthesis* **2003**, 337–339. (d) Miyaura, N.; Yamada, K.; Suzuki, A. *Tetrahedron Lett.* **1979**, 3437–3440. (e) Miyaura, N.; Suzuki, A. *Chem. Rev.* **1995**, *95*, 2457–2483. (f) Suzuki, A. *J. Organomet. Chem.* **1999**, *576*, 147–168.

(30) Djakovich, L.; Köhler, K.; de Vries, J. G. *The Role of Palladium Nanoparticles as Catalysts for Carbon-Carbon Coupling Reactions in Nanoparticles and Catalysis*, 1st ed.; Astruc, D., Ed.; Wiley-VCH: Weinheim, Germany, 2008; pp 303−348.

(31) Phan, N. T. S.; Van Der Sluys, M.; Jones, C. W. *Adv. Synth. Catal.* **2006**, *348*, 609–679.

(32) Yin, L. X.; Liebscher, J. *Chem. Rev.* **2007**, *107*, 133–173.

(33) (a) Xu, L.; Chen, W.; Xiao, J. *Organometallics* **2000**, *19*, 1123–1127. (b) Deshmukh, R. R.; Rajagopal, R.; Srinivasan, K. V. *Chem. Commun.* **2001**, 1544–1545. (c) Yang, X.; Fei, Z.; Zhao, D.; Ang, W. H.; Li, Y.; Dyson, P. J. *Inorg. Chem.* **2008**, *47*, 3292–3297.

(34) (a) Li, Y.; Hong, X. M.; Collard, D. M.; El-Sayed, M. A. *Org. Lett.* **2000**, *2*, 2385–2388. (b) Hu, J.; Liu, Y. B. *Langmuir* **2005**, *21*, 2121–2123. (c) Narayanan, R.; El-Sayed, M. A. *J. Am. Chem. Soc.* **2003**, *125*, 8340–8347. (d) Narayanan, R.; El-Sayed, M. A. *Langmuir* **2005**, *21*, 2027–2033. (e) Gallon, B. J.; Kojima, R. W.; Kaner, R. B.; Diaconescu, P. L. *Angew. Chem., Int. Ed.* **2007**, *46*, 7251–7254.

(35) Niembro, S.; Shafir, A.; Vallribera, A.; Alibés, R. *Org. Lett.* **2008**, *10*, 3215–3218.

(36) Mennecke, K.; Cecilia, R.; Glasnov, T. N.; Gruhl, S.; Vogt, C.; Feldhoff, A.; Vargas, M. A. L.; Kappe, C. O.; Kunz, U.; Kirschning, A. *Adv. Synth. Catal.* **2008**, *350*, 717–730.

(37) (a) Marck, G.; Villiger, A.; Buchecker, R. *Tetrahedron Lett.* **1994**, *35*, 3277–3280. (b) Tagata, T.; Nishida, M. *J. Org. Chem.* **2003**, *68*, 9412–9415. (c) Arvela, R. K.; Leadbeater, N. E. *Org. Lett.* **2005**, *7*, 2101–2104. (d) Sajiki, H.; Kurita, T.; Kozaki, A.; Zhang, G.; Kitamura, Y.; Maegawa, T.; Hirota, K. *Synthesis* **2005**, 537–542. (e) Maegawa, T.; Kitamura, Y.; Sako, S.; Udzu, T.; Sakurai, A.; Tanaka, A.; Kobayashi, Y.; Endo, K.; Bora, U.; Kurita, T.; Kozaki, A.; Monguchi, Y.; Sajiki, H. *Chem.−Eur. J.* **2007**, *13*, 5937–5943.

(38) (a) Heidenreich, R. G.; Köhler, K.; Krauter, J. G. E.; Pietsch, J. *Synlett* **2002**, 1118–1122. (b) Huang, J.; Wang, D.; Hou, H.; You, T. *Adv. Funct. Mater.* **2008**, *18*, 441–448.

(39) Köhler, K.; Heidenreich, R. G.; Krauter, J. G. E.; Pietsch, J. *Chem.−Eur. J.* **2002**, *8*, 622–631.

(40) Sakurai, H.; Tsukuda, T.; Hirao, T. *J. Org. Chem.* **2002**, *67*, 2721–2722.

(41) (a) Bigi, F.; Coluccia, S.; Maggi, S.; Martra, G.; Mazzacani, A.; Sartori, G. *Res. Chem. Intermed.* **2003**, *39*, 285–291. (b) Bedford, R. B.; Singh, U. G.; Walton, R. I.; Williams, R. T.; Davis, S. A. *Chem. Mater.* **2005**, *17*, 701–707. (c) Jana, S.; Dutta, B.; Bera, R.; Koner, S. *Inorg. Chem.* **2008**, *47*, 5512–5520. (d) Erathodiyil, N.; Ooi, S.; Seayad, A. M.; Han, Y.; Lee, S. S.; Ying, J. Y. *Chem.−Eur. J.* **2008**, *14*, 3118–3125.

Experimental Section

Catalyst Synthesis. GO was prepared by oxidation of graphite flakes (KFL 99.5, min 20% > 100 μm, Kropfmühl AG) according to the method described by Hummers and Offemann.[8] Graphite (15 g) was stirred in concentrated sulfuric acid (350 mL) at room temperature (rt), and sodium nitrate (7.5 g) was added. After 16 h, the mixture was cooled to 0 °C and potassium permanganate (45 g) was added. After 2 h, the green slurry was allowed to come to rt, and after being stirred for 3 h the whole batch was carefully poured into a 2-L beaker filled with ice-cold water. Subsequently, hydrogen peroxide (3%) was added in excess and the mixture was stirred overnight and then filtered. Workup was accomplished by several washings with a mixture of HCl/H_2O_2 (1:1, 5%) and filtration followed by several washings with water and centrifugation until the supernatant did not show anymore precipitation with $AgNO_3$ solution. Freeze-drying yielded a dark brown solid that was carefully powdered in a ball mill (60-μm mesh) with cooling. The obtained GO still had a sulfur content of 2% corresponding to 6% sulfate. This value was sufficiently low, and after Pd exchange and workup (see below) the sulfur content was reduced to 0. The ion exchange with Pd (i.e., the adsorption of Pd^{2+} ions by the functionalized GO) was achieved by dispersing GO (2.5 g) in water (200 mL). Subsequently, palladium acetate (250 mg, 1.1 mmol) was added and the mixture was vigorously sonicated for 5 min. Despite the low solubility of palladium acetate in water, cation exchange took place overnight. The suspension exhibited a slight vinegar smell, and after several washings with water and acetone the Pd^{2+}-GO was dried in vacuo at 40 °C and gently powdered through a 150-μm mesh regaining a water content of 4.5%. The powder density was roughly estimated to be 0.3 g cm^{-3}, and the Pd content amounted to 3.4%. The generation of Pd^0 nanoparticles within the GO support (sample Pd^0-CDG-H_2) was done by bubbling hydrogen through a suspension of Pd^{2+}-GO (0.5 g) in ethanol (100 mL) for 45 min with a flow of 40 mL min^{-1}. After evaporation of the solvent, the obtained material was again powdered through a 150-μm mesh, showing the same elemental composition as the Pd^{2+}-GO precursor. Partial reduction of Pd^{2+}-GO with hydrazine hydrate (sample Pd^0-CDG-N_2H_4) was performed as follows. A volume of 0.16 mL (165 mg, 3.3 mmol, 48.5 equiv of wrt Pd) of hydrazine hydrate (99.9% N_2H_5OH) was added to a suspension of Pd^{2+}-GO (0.2 g) in water (50 mL). After being stirred overnight, the grayish slurry was centrifuged and washed with water several times. The residue was then dried in vacuo at 40 °C and gently powdered through a 150-μm mesh, regaining a water content of 0.5%. The powder density was roughly estimated to be 0.3 g cm^{-3}, and the Pd content amounted to 3.4%. Sample Pd^0-CDG-EXP was obtained by placing Pd^{2+}-GO (0.5 g) in a Schlenck tube under an argon atmosphere and heating the material with a Bunsen burner to 500−600 °C for 2 min. Expansion of the GO support took place and yielded a sootlike material with a powder density of approximately 0.01 g cm^{-3} and a Pd content of 6.0%. All catalysts were not dried and were stored at rt in air to allow for easy handling.

Characterization of the Catalysts. The palladium content of the samples was determined by digestion of the samples in hot aqua regia followed by analysis on an atom absorption spectrometer (AAS) Vario 6 by Jena Analytics. Before elemental analysis on a VarioEL by Elementaranalysensysteme GmbH, the catalysts were dried in vacuo for 16 h and WO_3 was added. Thermogravimetric analyses (TGA) were performed on an STA 409 thermobalance by Netzsch under a nitrogen flow (75 mL min^{-1}) with a heating rate of 1 °C min^{-1}. The surface area was measured using the Brunauer, Emmet, and Teller (BET) method[57] on a Porotec Sorptomatic 1990 and by methylene blue (MB) adsorption. The MB technique was applied according to McAllister et al.[2] with some modifications. Four milligrams of the material was sonicated for 60 min in 100 mL of an aqueous solution of MB (0.04 mg L^{-1}) with sodium hydroxide (1.000 mL, 0.1 N). Following this, the remaining MB concentration was determined via UV−vis spectroscopy (absorption measured at 246 nm) after centrifugation. The reported value of 2.54 m^2 of surface area per milligram of MB adsorbed was used to calculate the surface area of the samples. Nanoparticles were characterized by transmission electron microscopy (TEM) in suspension on a 200-μm mesh Cu grid and as a microtome cut of the samples embedded in epoxy resin with a LEO CEM 912 operating at 120 kV. Particle size was determined counting at least 200 particles from different images by the aid of iTEM computer software by OlympusSIS. The morphology of the materials was observed via environmental scanning electron microscopy (ESEM) in an Electroscan ESEM 2020. An acceleration voltage of 23 kV was applied, and the samples were coated with gold/palladium before analyses. The wide-angle X-ray scattering (WAXS) measurements were carried out on a Siemens D 5000 diffractometer at 40 kV and 30 mA with Cu K_α radiation in the 2θ range from 1° to 100° (step size 0.0156°, step time 1 s, transmission rotation and detection by a Braun PSD ASA S). Interplanar distances were calculated using Bragg equation. X-ray photoelectron spectra (XPS) were recorded on a Perkin-Elmer PHI ESCA System. X-ray source was a Mg standard anode (1253.6 eV) at 12 kV and 300 W. Samples were dried at rt in a high vacuum overnight, compressed with 75 MPa, and again dried in a high vacuum overnight, and the surface was sputtered with argon for 20 s before measurements.

General Procedure for the Kinetic Measurements. The vessels of the ASW 2000 were charged with palladium catalyst (x μmol, y mol %), sodium carbonate (106 mg, 1 mmol, 2 equiv), boronic acid (0.55 mmol, 1.1 equiv), and aryl bromide (0.50 mmol, 1 equiv). After automatic addition to each vessel of ethanol (2 mL) and water (2 mL), the mixtures were shaken (600 min^{-1}) at rt. After 10, 30, 60, 120, 180, 240, 300, 360, 420, and 1440 min, small probes (20 μL) were taken and given in HPLC vessels with acetonitril (950 μL + 30 μL acetic acid). From these probes, the conversion was calculated via HPLC.

General Procedure for the Suzuki Reaction. A pressure tube was charged with boronic acid (0.55 mmol, 1.1 equiv), sodium carbonate (106 mg, 1 mmol, 2 equiv), aryl bromide (0.5 mmol, 1 equiv), and palladium catalyst **2** (4.0 mg, 1.25 μmol, 0.25 mol %). Ethanol (2 mL) and water (2 mL) were added, and the flask was sealed with a Teflon screw cap and stirred in a preheated oil bath (80 °C) for the time indicated, followed by taking 10 μL of the mixture for HPLC analysis. After cooling to rt, the mixture was filtered over a small column of silica gel/kieselgur, and the column was washed with DCM (10 mL). The product was extracted into the organic phase (2 × 10 mL DCM), the united organic phases were dried over $MgSO_4$ and filtered, and the solvent was removed under reduced pressure. In some cases, the pure product was obtained after column chromatography (d = 2.5 cm, h = 10 cm, CH/EE 4:1).

Results and Discussion

Synthesis and Characterization of the CDG Catalysts. The GO obtained by the Hummers−Offemann method[8] had an oxygen content of 41 wt %. This composition can be described in good accordance with the empirical formula $C_6H_2O_3$ proposed by Boehm et al.[9] This highly oxidized carbonaceous material was dispersed in water, and after addition of palladium acetate ion exchange took place overnight. After catalyst recovery, the palladium content of the obtained Pd^{2+}-GO **2** amounted to 3.4 wt % (0.32 mmol g^{-1}) as verified by AAS. Palladium(II) supported on GO was reduced to produce a variety of catalysts comprising palladium(0) nanoparticles and CDG. The obtained catalysts are listed in Table 1.

(42) (a) Augustine, R. L.; O'Leary, S. T. *J. Mol. Catal.* **1992**, *72*, 229–242. (b) Biffis, A.; Zecca, M.; Basato, M. *Eur. J. Inorg. Chem.* **2001**, 1131–1133.

(43) (a) Djakovitch, L.; Koehler, K. *J. Am. Chem. Soc.* **2001**, *123*, 5990–5999. (b) Dams, M.; Drijkoningen, L.; Pauwels, B.; Van Tendeloo, G.; De Vos, D. E.; Jacobs, P. A. *J. Catal.* **2002**, *209*, 225–236.

Table 1. Catalysts Investigated in the Suzuki−Miyaura Coupling Reaction Including Conventional Pd/C **1** as Benchmark

sample	composition[a]	oxygen content[b] (wt %)	Pd loading[c] (wt %)	particle diameter[d] (nm)	surface area MB[e] ($m^2\ g^{-1}$)	surface area BET[f] ($m^2\ g^{-1}$)
Pd/C **1**[g]		n.d.	10	n.d.	n.d.	820
Pd^{2+}-GO **2**	$C_6H_{1.9}O_{3.2}$	41	3.4	4 ± 1[h]	1050 (430)	n.d.
Pd^0-CDG-H_2 **3**	$C_6H_{0.9}O_{1.7}$	28	3.4	7 ± 2	350 (250)	n.d.
Pd^0-CDG-N_2H_4 **4**	$C_6H_{1.2}O_{1.5}$	25	3.5	54 ± 28	410 (130)	220
Pd^0-CDG-EXP **5**	$C_6H_{0.5}O_{1.1}$	19	6.0	3 ± 1	890 (410)	650

[a] Calculated from elemental analysis. [b] Calculated from elemental analysis wrt the support material (CH) only. [c] Measured by AAS after digestion of the wet samples in aqua regia. [d] Average size and standard deviation as measured by TEM analysis. [e] Modified methylene blue adsorption technique. Values in parentheses were obtained from measurements at pH ≤ 7. [f] BET adsorption isotherm. [g] 10% Pd on activated charcoal (Sigma-Aldrich, product No. 75990). [h] Particles generated in situ (i.e., TEM analysis was performed with the recollected catalyst).

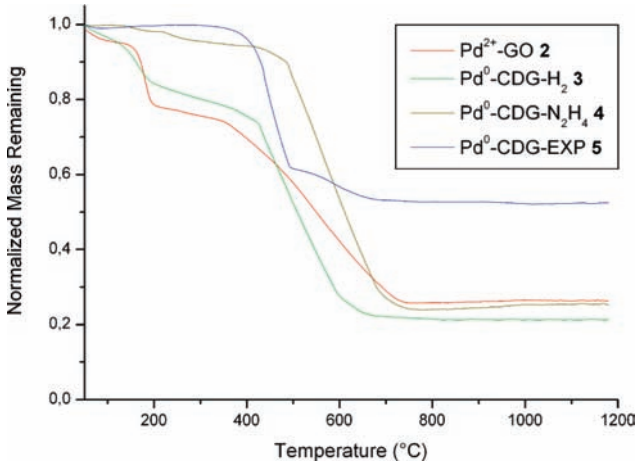

Figure 1. Thermogravimetric analysis of the catalysts under nitrogen.

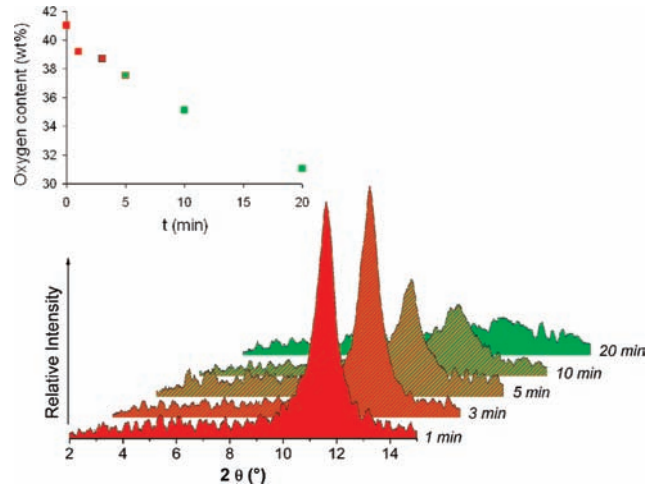

Figure 2. Interlayer distance (bottom) and oxygen content (top) (wrt to CH only) monitored by WAXS and elemental analysis, respectively, during reduction of Pd^{2+}-GO **2** with H_2.

Reduction of a Pd^{2+}-GO **2** suspension in ethanol with H_2 generated Pd^0 nanoparticles with a diameter of 5−9 nm (sample Pd^0-CDG-H_2 **3**). The GO support was also reduced to a CDG material containing 28 wt % oxygen. When reducing an aqueous suspension of Pd^{2+}-GO **2** with hydrazine hydrate, Pd^0 clusters of 26−82 nm in diameter were produced. This was accompanied by partial reduction of the GO support to a CDG with an oxygen content of 25 wt % (sample Pd^0-CDG-N_2H_4 **4**). "Regraphitization" was observed accompanied by precipitation of a shiny layer of less hydrophilic CDG. In contrast to the reports of Stankovich et al., no remaining nitrogen was detected in this material.[19] Thermal expansion of Pd^{2+}-GO accompanied by thermal reduction accounted for the formation of a sootlike carbon material consisting of agglomerates of CDG with an oxygen content of 19 wt % (sample Pd^0-CDG-EXP **5**). Thermal degradation of the different catalysts by means of TGA exhibits very different degradation profiles as expected for the degree of functionalization of each sample (Figure 1). The reduction of the nonreduced Pd^{2+}-GO **2** took place in two distinct steps with an onset temperature of 165 and 350 °C accounting for 22 and 60% mass loss, respectively (exclusive of water). With decreasing oxygen content of the samples the first degradation step diminished and onset temperatures were shifted to higher values.

The thermal "regraphitization" of GO is accompanied by the release of CO, CO_2, and steam.[2,15] Hence, mass loss in TGA cannot be correlated with the carbon content of the samples. Presumably, the decomposition of different types of oxygen-containing functional groups is responsible for the different degradation steps. This is in accordance with IR data of sample Pd^0-CDG-EXP **5** where only a weak band at 1725 cm^{-1} could be assigned to C═O groups. Signals indicating epoxy and carboxyl groups were absent, thus suggesting that these functional groups were decomposed in the first degradation step. It was found that the oxygen content (i.e., the degree of reduction of Pd^0-CDG-H_2 **3**) could easily be adjusted by simply varying the reaction time. During the reduction of Pd^{2+}-GO **2** with H_2, aliquots were withdrawn from the suspension, spray-dried, and subsequently analyzed by elemental analysis and WAXS. The results are shown in Figure 2.

The layered structure of the GO support was destroyed during reduction as the pendant functional groups were decomposed and Pd nanoparticles with diameters larger than the GO interlayer distance were formed. Obviously, the GO support was reduced to a CDG material with lower oxygen content and lower degree of functionalization. Morphology of the catalysts was examined by ESEM and WAXS. Pd^{2+}-GO **2** and the partially reduced samples Pd^0-CDG-H_2 **3** and Pd^0-CDG-N_2H_4 **4** consisted of platelets, the latter showing a slightly exfoliated structure of agglomerated GO and CDG layers, respectively (Figure 3).

However, in the WAXS diffractogram the characteristic [001] reflex of a layered material was absent in all reduced samples as nonuniform expansion in the *c*-axis of the support took place (Figure 4). Reflexes in the WAXS pattern of sample Pd^0-CDG-N_2H_4 **4** can be attributed to cubic palladium.

In GO remaining crystalline features from graphite such as strong hk0 reflexes can be observed. Notably, in the CDG samples these reflexes disappeared completely, attesting to an unordered structure of the CDG. A weak reflex at 21.5° (d = 4.13 Å) appears in the diffractogram of the thermally reduced Pd^0-CDG-EXP **5**. Although expansion and delamination of the layers during synthesis lead to a rather amorphous material, this can be ascribed to the formation of "regraphitized" carbon

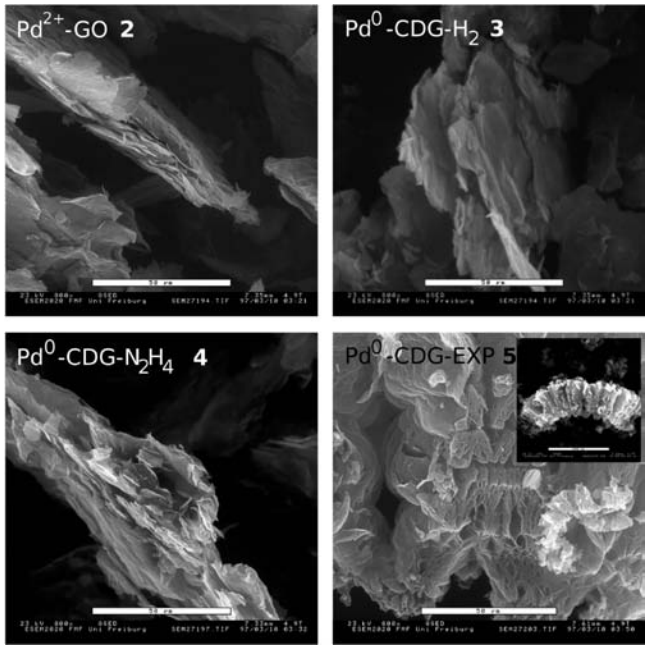

Figure 3. ESEM images of the catalysts in 800-fold magnification (the scale bar is 50 μm). The inset in the image of sample Pd^0-CDG-EXP **5** shows a particle at 175-fold magnification (scale bar is 250 μm). The typical accordion structure of this particle due to expansion of the layers can be observed.

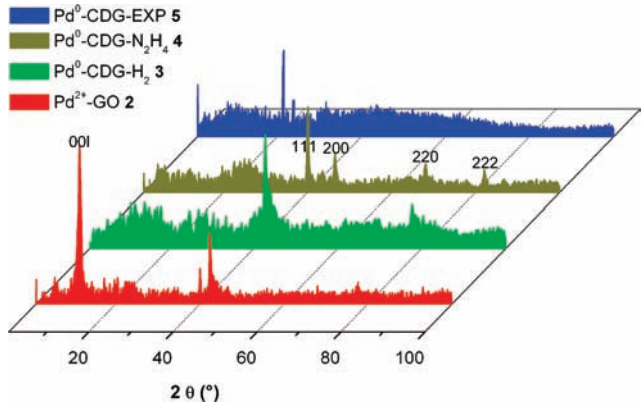

Figure 4. WAXS patterns of GO- and CDG-Pd composites. The broad peak between 20 and 30° can be attributed to remaining reflexes of the capillary tube material. The *d*-spacings of >1.5 nm could not be detected because of the limited resolution (due to weak reflexes of the materials and the insufficient low-angle resolution of the instrument).

regions. This is well-known for different types of soot where a weak [002] interference stems from randomly arranged parallel graphene layer stacks exhibiting larger *d*-spacings than pristine graphite.[44] Stacking is due to van der Waals attractive interactions. As a result, selected area electron diffraction (SAED) eventually shows sharp reflexes of ordered regions (see inset of Figure 5). In addition, "regraphitization" can be enhanced by compression of the material. WAXS patterns of tablets formed by compression of the reduced samples with 75 MPa show a broad peak between 17 and 30° owing its highest maximum to the [002] reflex of hexagonal carbon with a *d*-spacing of 3.37 Å. It has to be noted that thermally reduced GO is different from commercially available expanded graphite produced from graphite intercalation compounds. The latter also

(44) Hofmann, U.; Wilm, D. *Z. Elektrochem.* **1936**, *42*, 504–522.

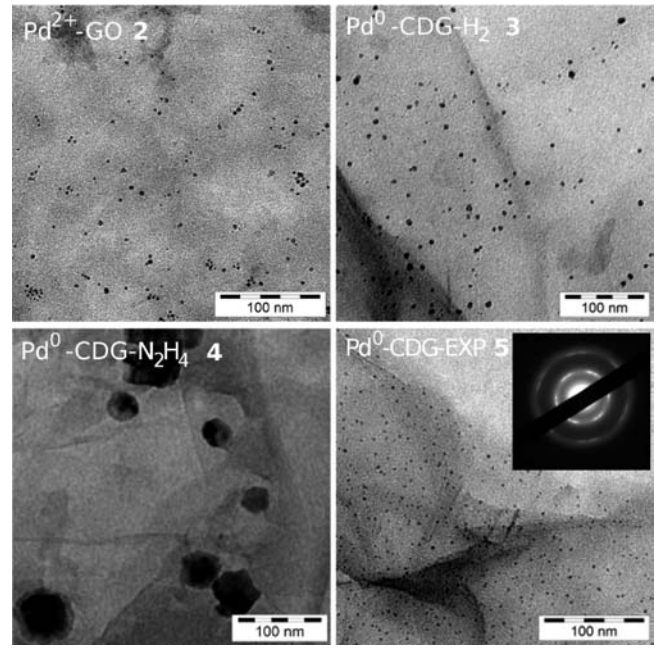

Figure 5. TEM images of the catalysts. Nanoparticles formed simultaneously during the reduction of the GO. Palladium nanoparticles in sample Pd^{2+}-GO **2** were generated in situ during the Suzuki−Miyaura coupling reaction. The SAED in the inset shows a hexagonal pattern that can be ascribed to "regraphitized" regions.

shows particles with wormlike structures but with stacks of unchanged graphite crystallites having sharp X-ray diffraction peaks. Moreover, the typical surface area of these materials is rather low (<100 $m^2\ g^{-1}$), whereas sample Pd^0-CDG-EXP **5** inhibits a much higher specific surface area of 650 $m^2\ g^{-1}$ according to BET measurements. The results of the modified MB adsorption technique were approximately double the surface area values obtained by the BET method. This is possibly due to agglomeration of the dry powder and its exfoliation in alkaline aqueous suspension, respectively. The Pd dispersion (i.e., the average Pd crystallite size of the catalysts) could not be determined by these adsorption experiments. However, dispersion was determined by measuring the particle diameter via TEM. Excitingly, thermal reduction of the GO support was accompanied by the formation of highly dispersed nanoparticles with an extremely narrow size distribution of 3.3 ± 0.7 nm (sample Pd^0-CDG-EXP **5** in Figure 5).

Moreover, the palladium nanoparticles had a spherical shape as confirmed by microtome cuts of the embedded samples. Pd^0 nanoparticles generated in situ and by hydrogen were also quasi-spherical and dispersed all over the carbon support. Those generated by hydrogen exhibited a wider size distribution of 7 ± 2 nm. However, nanocrystallites of cubic Pd generated by the hydrazine reduction accumulated in several spots that were randomly distributed in the CDG support. XPS measurements confirmed the findings of the WAXS analysis of this sample; nanocrystallites consisted of Pd^0. The peaks occurring in the XP spectra of nonreduced sample Pd^{2+}-GO also matched literature values for Pd^{2+} ions.[45] Nevertheless, the spectrum of the thermally reduced sample Pd^0-CDG-EXP **5** showed a broad signal. This revealed that the nanoparticles observed by TEM consisted of both Pd^0 and Pd oxides.

Catalyst Screening in C−C Coupling Reactions. The Suzuki−Miyaura reaction is one of the most widely used synthetic protocols in modern chemistry and in industrial application.[46]

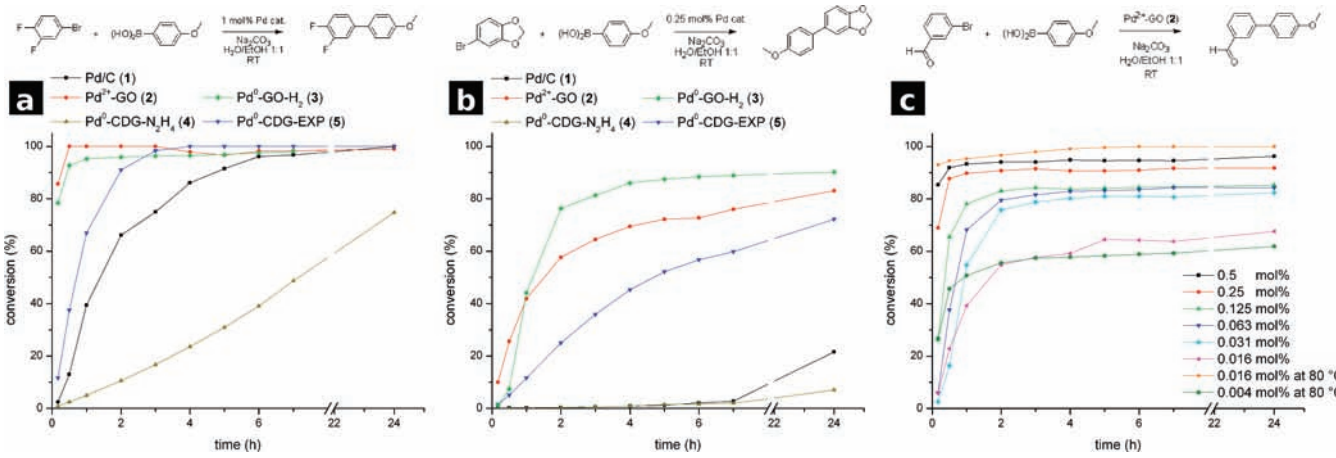

Figure 6. Catalyst screening in the Suzuki−Miyaura reaction. Comparison of Pd-GO/CDG catalysts **2**−**5** and Pd/C **1**. (a) Coupling of 4-methoxyphenylboronic acid and 4-bromo-1,2-difluorobenzene (1 mol %). (b) Coupling of 4-methoxyphenylboronic acid and 4-bromo-1,2-(methylene dioxy)benzene (0.25 mol %). (c) Coupling of 4-methoxyphenylboronic acid and 3-bromobenzaldehyde with different Pd amounts (catalyst Pd^{2+}-GO **2**).

The organo boronic acids are largely unaffected by the presence of water, tolerate a broad range of functional groups, and yield nontoxic byproduct. In recent years, the focus of the research has been directed on the synthesis of heterogeneous catalytic systems.[37,40,47,48] These systems show the same or even higher activities than homogeneous catalysts, do not require working under an inert atmosphere, and are very easy to recover, though the activities often drop in recycling experiments.[40,48]

The supported Pd-GO/CDG catalysts described above were applied to the Suzuki−Miyaura coupling reaction. Commercially available Pd on charcoal (Pd/C) **1** was used as reference. All catalysts were easily suspended in the solvent with stirring or shaking but allowed for facile separation from the reaction mixture when at rest. To establish an approximate activity ranking among the catalysts, a Suzuki−Miyaura coupling reaction with reactive substrates and 1 mol % Pd was monitored at rt (Figure 6a).

The highest activity was reached with Pd^{2+}-GO **2** and the H_2-reduced derivative Pd^0-CDG-H_2 **3** followed by Pd^0-CDG-EXP **5** and Pd/C **1**. After 30 min, the reaction shows complete conversion with catalyst **2**, in comparison to 93% with **3,** 38% with **5**, and only 17% with Pd/C **1**. All catalysts lead to complete conversion except for the hydrazine-reduced sample Pd^0-CDG-N_2H_4 **4**. This catalyst displayed the lowest activity and 77% conversion after 24 h. On the basis of these findings, a Suzuki−Miyaura coupling with a less electrophilic and thus less reactive aryl bromide and with lower Pd concentration of 0.25 mol % was performed (Figure 6b). Here, the difference in activity between the catalysts is much more conspicuous. While catalysts **2**, **3**, and **5** yielded the coupling product with 83, 90, and 72% conversion, only 21% was achieved with Pd/C **1**. Again, Pd^0-CDG-N_2H_4 **4** showed the lowest activity, affording 8% of product after 24 h. Subsequently, the maximum enhancement in activity was investigated by lowering the Pd loadings. Six different amounts of Pd were applied to the coupling reaction of 3-bromobenzaldehyde with 4-methoxyphenylboronic acid and Pd^{2+}-GO **2** at rt (Figure 6c). With the highest loading of 0.5 mol % the reaction was completed after 1 h with a yield of 93% of product. Decreasing the Pd concentration to 0.03 mol % still gave a conversion of 80% after 4 h. By further decreasing the amount of Pd to 0.016 mol %, the conversion dropped substantially to 65%. However, the activity of the catalyst is quite remarkable at concentrations that low. When the same Pd concentration was applied at 80 °C, the reaction was surprisingly fast, converting 93% of the halo aryl after 10 min. When 0.004% Pd was applied at 80 °C, the system remained highly active, converting 27% of the halo aryl after 10 min. This results in a turnover number (TON) of 6700 and a turnover frequency (TOF) of 39 000 h^{-1}. To the best of our knowledge, this is the highest TOF observed in the Suzuki−Miyaura reaction with a heterogeneous catalyst. Heterogeneity of the catalytic systems was confirmed by determining the Pd leaching (mechanistic aspects are discussed below). After complete reaction, samples from reaction mixtures with 1 mol % Pd were analyzed by ICP-AAS, showing very low leaching of 1.1 ppm in the case of the highly active catalyst Pd^{2+}-GO **2** and values of <1 ppm for the Pd^0-CDG catalysts **3**−**5**.

Furthermore, the scope of the Suzuki−Miyaura reaction with Pd^{2+}-GO **2** was thoroughly investigated (Table 2). The reactions proceeded extraordinarily well with a wide range of aryl bromides containing electron-donating groups (**7**−**11**), electron-withdrawing groups (**12**−**18**), or aromatic substituents such as that in 2-bromonaphthalene (**19**−**21**). However, coupling reaction of 2-bromopyridine with both boronic acid leads only to modest conversion (**20a**). In most cases, the formation of homocoupling products was not observed and never exceeded 4%.

In addition, the recyclability of the catalysts was studied in the coupling reaction forming 3-(4′-methoxyphenyl)benzaldehyde **12a** at 80 °C and with 0.25 mol % Pd. With Pd^{2+}-GO **2**, completion of the reaction was accomplished after 20 min in the first run. The activity slightly dropped in the next two runs, dramatically dropping in the fourth, showing just 19% conversion (Table 3).

(45) (a) Briggs, D.; Seah, M. P. *Practical Surface Analysis: By Auger and X-ray Photoelectron Spectroscopy*, 2nd ed.; Wiley: Chichester, U.K., 1990; Vol. 1. (b) Kumar, G.; Blackburn, J. R.; Albridge, R. G.; Moddeman, W. E.; Jones, M. M. *Inorg. Chem.* **1972**, *11*, 296–300.
(46) Tsuji, J. *Palladium Reagents and Catalysts: New Perspectives for the 21st Century*, 1st ed.; Wiley: Chichester, U.K., 2004.
(47) (a) LeBlond, C. R.; Andrews, A. T.; Sun, Y.; Sowa, J. R. *Org. Lett.* **2001**, *3*, 1555–1557. (b) Kitamura, Y.; Sako, S.; Udzu, T.; Tsutsui, A.; Maegawa, T.; Monguchi, Y.; Sajiki, H. *Chem. Commun.* **2007**, 5069–5071.
(48) (a) Arcadi, A.; Cerichelli, G.; Chiarini, M.; Correa, M.; Zorzan, D. *Eur. J. Org. Chem.* **2003**, *2003*, 4080–4086. (b) Lysén, M.; Köhler, K. *Synthesis* **2006**, 692–698.

Table 2. Suzuki−Miyaura Reactions of Different Aryl Bromides with 0.25 mol % Pd^{2+}-GO **2**

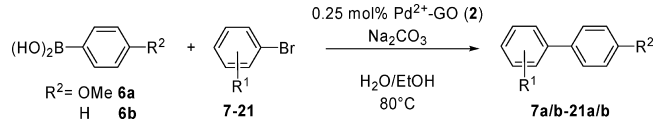

Arylbromide	R^2	Product	Time	Conversion	Yield
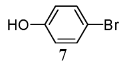 7	-OMe	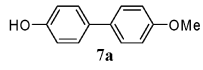 **7a**	24 h	93%	84%
	-H	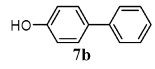 **7b**	17 h	100%	96%
 **8**	-OMe	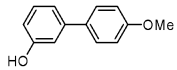 **8a**	24 h	96%	86%
	-H	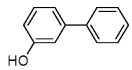 **8b**	24h	94%	87%
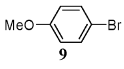 **9**	-OMe	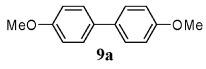 **9a**	4 h	100%	81%
	-H	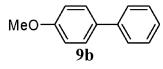 **9b**	4 h	100%	99%
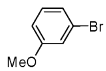 **10**	-OMe	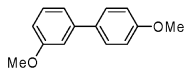 **10a**	4 h	100%	87%
	-H	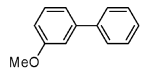 **10b**	4 h	96%	96%
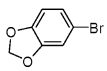 **11**	-OMe	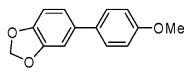 **11a**	8 h	97%	91%
	-H	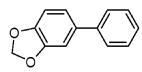 **11b**	8 h	98%	97%
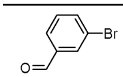 **12**	-OMe	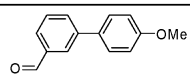 **12a**	4 h	100%	84%
	-H	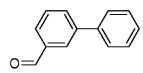 **12b**	4 h	100%	98%
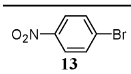 **13**	-OMe	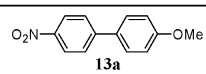 **13a**	4 h	100%	99%
	-H	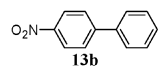 **13b**	4 h	100%	100%

Arylbromide	R^2	Product	Time	Conversion	Yield
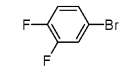 **14**	-OMe	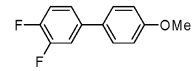 **14a**	4 h	100%	100%
	-H	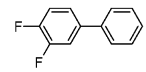 **14b**	4 h	100%	97%
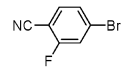 **15**	-OMe	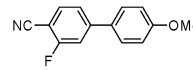 **15a**	4 h	100%	94%
	-H	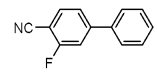 **15b**	10 h	100%	92%
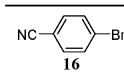 **16**	-OMe	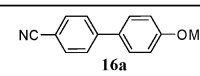 **16a**	4 h	100%	89%
	-H	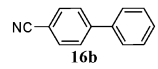 **16b**	4 h	100%	96%
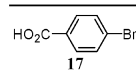 **17**	-OMe	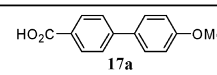 **17a**	24 h	86%	83%
	-H	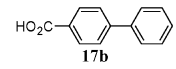 **17b**	24 h	93%	94%
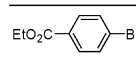 **18**	-OMe	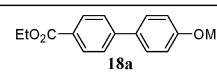 **18a**	4 h	100%	93%
	-H	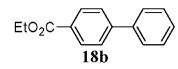 **18b**	4 h	100%	87%
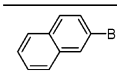 **19**	-OMe	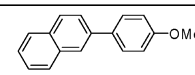 **19a**	4 h	100%	96%
	-H	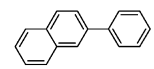 **19b**	4 h	100%	94%
20	-OMe	**20a**	24 h	36%	
	-H	**20b**	24 h	34%	
21	-H	**21b**	4 h	100%	100%

The Pd^0 nanoparticles that formed in situ on the Pd^{2+}-GO catalyst **2** (cf. Figure 5) agglomerated and accumulated in several spots on the support in the course of recycling. However, formation of Pd black did not take place. Reuse of the Pd^0-CDG catalysts **3**−**5** was accompanied by a substantial loss in activity in the second run already (10−27% conversion). This behavior cannot be explained by leaching during the reaction as the Pd amount in the reaction mixture after the first run exhibited very low values of <1 ppm. The activity in recycling experiments strongly depended on the recycling procedure.

Table 3. Recycling Experiment with Pd^{2+}-GO **2**[a]

run	conversion (%)[b]
1	100
2	83
3	74
4	19

[a] Formation of 3-(4′-methoxyphenyl)benzaldehyde was catalyzed with a total TON of 1100. [b] This is in line with the results found in TEM analyses (Figure 7).

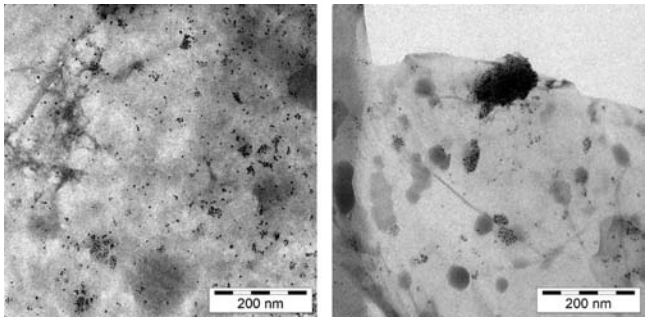

Figure 7. Pd particles formed on catalyst Pd^{2+}-GO **2** after the first run (left) and fourth run (right). Agglomeration of the particles can be observed.

Results described above were obtained when centrifugation was applied to separate the catalysts from the reaction mixture and after washings with water and diethylether. However, simple filtration followed by washings in the same manner led to a massive decrease in activity in the second run (4−6%). This is in contrast to the new addition of substrates to the reaction mixture after the completed first run, which gave again 100% conversion.

Many correlated aspects have to be taken into account when commenting on the reasons for the different activities among the catalysts. The shape and size of the nanoparticles and their size distribution (i.e., the Pd dispersion) are the most easily understandable aspect. Regardless of the exact mechanism of the reaction, a high surface area is expected to increase the activity of a heterogeneous catalyst. Good accessibility to the catalytic particles by the reagents is an additional premise, and thus the surface area of the support also plays an important role. From this it follows that the catalysts having the smallest Pd nanoparticles and highest specific surface areas, namely Pd^{2+}-GO **2** and Pd^0-CDG-EXP **5**, should display the highest activities. This is not true for the latter, which can be ascribed to the nature of the particles. They consist of a mixture of Pd oxides and Pd^0, and thus not all the Pd is available for the coupling reaction, which is catalyzed by Pd^0 species. Moreover, Pd oxides behave rather inertly at the applied reaction conditions and leaching of Pd^0 is negligible. In contrast, Pd^0 formation on the catalyst Pd^{2+}-GO **2** via in situ reduction by the solvent under basic conditions leads to the highest Pd dispersion. The dispersion is supposed to be even higher during the reaction than suggested by the final particle size measured after complete reaction. It is obvious from the foregoing that Pd^0-CDG-N_2H_4 **4** accounts for the lowest activity. Furthermore, the role of the support has to be considered. In general, one of the main influences of the support is attributed to its acidity or basicity.[32] The extent of this effect in turn varies with the characteristics of the reagents. In conclusion, the different kinetic profiles of catalyst Pd^{2+}-GO **2** and Pd^0-CDG-H_2 **3** are possibly due to the dissimilar degree of derivatization (41 vs 28% oxygen content). This is corroborated by recent studies by Han et al., who proposed a model for the oxygen-promoted ligand-free Suzuki−Miyaura coupling.[49] The findings described above are in line with the poor performance of commercially available Pd/C **1**. Of course, the impregnation method (i.e., the fabrication procedure) has a strong impact on the activity of Pd/C.[39] However, the high Pd dispersion in Pd/C is in sharp contrast to the low activities, which are probably due to the inert behavior of the support. It is worth noting that the Pd-GO/CDG catalysts did not show a decrease in activity after six months, despite their high degree of functionalization. Moreover, they were stored in air at rt to allow for easy handling.

Scheme 1. Three-Phase Test[a]

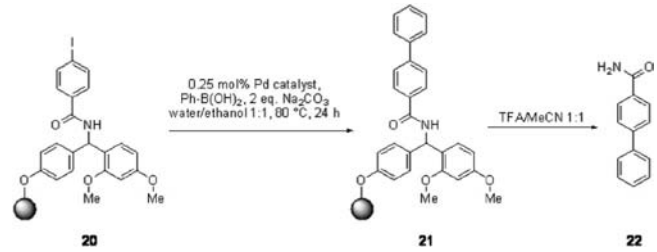

[a] Suzuki reaction with a solid-phase-bound aryl iodide. The conversion was determined by HPLC after cleavage from the solid support.

To shed more light on the mechanism of the Suzuki−Miyaura coupling with the heterogeneous Pd-GO/CDG catalysts,[31] three-phase tests[50,51] and filtration experiments[52] were carried out. In the three-phase test, a solid-phase-bound aryl iodide is subjected to the reaction conditions (Scheme 1).

If the catalytic species is truly immobilized, the spatial separation from the iodide will prevent any conversion, while a soluble catalyst can reach the substrate by diffusion and thus effect conversion. The experiment was carried out with Pd/C **1**, Pd^{2+}-GO **2**, and Pd^0-CDG-EXP **5** in the presence and in the absence of 4-bromophenol as a soluble substrate. In both experiments for all three catalysts, more than 90% conversion of the solid-phase-bound iodide was observed. These results suggest that the catalysts are operating by a soluble catalytic species and do not depend on a soluble aryl halide for generation of the active species from the precatalyst. Further experimental support was provided by the observation that the reaction continues after hot filtration of the reaction mixture and leads to nearly the same conversion (Figure 8).

Upon completion of the reaction and cooling to rt, the Pd species were probably redeposited on the support, which would be in accordance with the low Pd leaching. Nevertheless, it is also conceivable that the support acts as a reservoir and only a small fraction of active catalytic species is released into the solution. These results are in accordance with the widespread hypothesis that Pd nanoparticles function as a reservoir. Only a small amount of metal goes into solution as Pd^0 atoms and catalyzes the reaction, returning to the solid support after completion of the transformation (dissolution−redeposition mechanism).[30,39,51,53] This is not contradictory to the role of the support discussed above since the reaction can still be

(49) Han, W.; Liu, C.; Jin, Z. L. *Org. Lett.* **2007**, *9*, 4005–4007.
(50) (a) Collman, J. P.; Kosydar, K. M.; Bressan, M.; Lamanna, W.; Garrett, T. *J. Am. Chem. Soc.* **1984**, *106*, 2569–2579. (b) Smith, M. D.; Stepan, A. F.; Ramarao, C.; Brennan, P. E.; Ley, S. V. *Chem. Commun.* **2003**, 2652–2653. (c) Tzschucke, C. C.; Bannwarth, W. *Helv. Chim. Acta* **2004**, *87*, 2882–2889.
(51) Davies, I. W.; Matty, L.; Hughes, D. L.; Reider, P. J. *J. Am. Chem. Soc.* **2001**, *123*, 10139–10140.
(52) Sheldon, R. A.; Wallau, M.; Arends, I.; Schuchardt, U. *Acc. Chem. Res.* **1998**, *31*, 485–493.

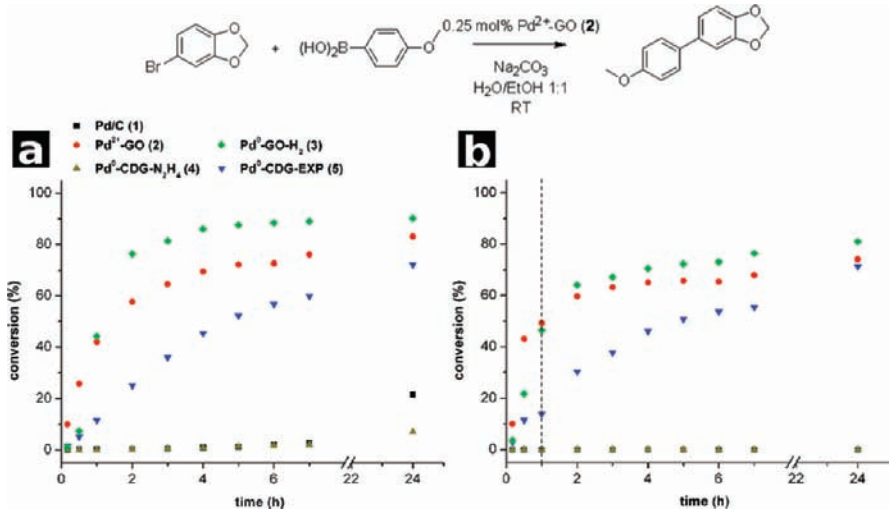

Figure 8. Filtration experiment. Formation of 4-methoxy-3′,4′-methylenedioxybiphenyl. (a) Without filtration. (b) Filtration of the catalyst from the reaction mixture after 60 min.

influenced positively by homogeneous active species interacting with the surface of GO/CDG. Filtration experiments give further evidence. After filtration of the catalysts from the reaction mixture, a distinct decrease in activity can be observed. Therefore, it can be speculated that the reaction proceeds via a support-aided homogeneous mechanism.

Conclusions

In summary, immobilization of Pd^{2+} on graphite oxide (GO) via cation exchange and subsequent chemical reduction afforded Pd^0 nanoparticles and chemically derived graphenes (CDG). The (GO)-Pd and the (CDG)-Pd catalysts were successfully applied to the Suzuki−Miyaura coupling reaction. These novel heterogeneous catalysts were readily available and easy to handle as they are stable in air. Extraordinary high activities with turnover frequencies (TOF) of up to 39 000 h^{-1} and very low leaching make them an attractive alternative to commercially available Pd catalysts such as Pd on charcoal. Reuse of the catalysts can be achieved, albeit with loss in activity depending on the recycling procedure. However, recovery of the noble metal is possible because of very low leaching.

The present work shows the outstanding versatility of GO as a starting material for transition-metal nanoparticle supports. By simple variation of the reduction methods and procedure parameters size and shape of the nanoparticles and the functionalization of the support can be varied. Nevertheless, for a profound understanding of the structure−activity relationship of Pd-GO/CDG catalysts further work has to be done. Currently, the rediscovery of GO and its derivatives has led to a much better understanding of its nature and processabilty. Recent progress such as the selective ion passage through functionalized graphene pores[54] or the Langmuir−Blodgett assembly of GO[55] offers attractive new opportunities for designing highly active catalysts with hierarchic architectures and tailored nanocatalysts.[56]

Acknowledgment. We gratefully acknowledge financial support by the DFG Priority Research Program SFB428. TEM images were measured by Dr. Ralf Thomann.

Note Added after ASAP Publication. After ASAP publication on May 25, 2009, Table 2 was reprocessed to better display the data. The corrected version was published May 27, 2009.

Supporting Information Available: Characterization of GO and the Pd-GO/CDG catalysts and experimental procedures and spectroscopic data for all Suzuki coupling products. This material is available free of charge via the Internet at http://pubs.acs.org.

JA901105A

(53) (a) De La Rosa, M. A.; Velarde, E.; Guzmán, A. *Synth. Commun.* **1990**, *20*, 2059–2064. (b) Reetz, M. T.; de Vries, J. G. *Chem. Commun.* **2004**, 1559–1563. (c) Gaikwad, A. V.; Holuigue, A.; Thathagar, M. B.; ten Elshof, J. E.; Rothenberg, G. *Chem.−Eur. J.* **2007**, *13*, 6908–6913.

(54) Sint, K.; Wang, B.; Král, P. *J. Am. Chem. Soc.* **2008**, *130*, 16448–16449.

(55) Cote, L. J.; Kim, F.; Huang, J. *J. Am. Chem. Soc.* **2009**, *131*, 1043–1049.

(56) Schlögl, R.; Abd Hamid, S. B. *Angew. Chem., Int. Ed.* **2004**, *43*, 1628–1637.

(57) Brunauer, S.; Emmett, P. H.; Teller, E. *J. Am. Chem. Soc.* **1938**, *60*, 309–319.